Malaysian Journal of Chemistry, 2023, Vol. 25(4), 62-72

Solid-Phase Extraction of Pb(II) Using Glutaraldehyde Crosslinked Chitosan/Carboxymethyl Cellulose

Muhammad Rizza Umami, Dwi Siswanta* and Mudasir Mudasir
Department of Chemistry, Faculty of Mathematics and Natural Sciences, Universitas Gadjah Mada, Sekip Utara Yogyakarta 55281, Indonesia
*****Corresponding author (e-mail: dsiswanta@ugm.ac.id)

Glutaraldehyde-crosslinked chitosan/carboxymethyl cellulose was synthesized as a sorbent for the solid-phase extraction (SPE) of Pb ions. This study optimized the SPE method for Pb^{2+} preconcentration. SPE parameters such as pH, sample concentration, loading and eluting flow rates, and reusability were investigated. The Pb^{2+} concentration retained in the sorbent was analysed using AAS (atomic absorption spectrometry), while the sorbent was characterized using FT-IR (Fourier transform infrared) spectroscopy and SEM-EDX (scanning electron microscope-energy dispersive x-ray). The optimum parameters for SPE were pH 6, an initial Pb concentration of 10 mg L^{-1} and flow rates for both loading and elution of 9 mL min^{-1}. The highest efficiency achieved under these optimum conditions was 98.98 %. However, this efficiency reduced with repeated sorbent usage to 82.34 % in the second cycle and 40.22 % in the fifth cycle.

Keywords: Chitosan; carboxymethyl cellulose; glutaraldehyde; crosslinking; solid-phase extraction

Received: January 2023; Accepted: February 2023

Heavy metals are commonly released into the environment through wastewater as pollutants which can be very dangerous to human health [1], [2]. A pollutant is any material in the environment that has undesirable consequences, affecting the environment's well-being, diminishing quality of life, and possibly causing death [3]. Such material must exceed an established tolerance limit, which could be either desirable or acceptable [4]. Therefore, the removal of heavy metals is essential since they can persist in water bodies (e.g., surface waters, groundwater and drinking water) and the food chain [5]. So far, various methods for heavy metal removal have been investigated [6]. These methods are mainly based on separation techniques aimed at purifying analytes from mixtures [7], such as precipitation, ion exchange, adsorption, electrodialysis and filtration [8]. Among these methods, adsorption is the most efficient, cost-effective and environmentally friendly [9].

Heavy metals with a high level of toxicity, such as lead (Pb), can cause severe nervous system problems [8]. As a trace metal, Pb may be present in plants, soil, food and water. Industrial waste from sectors including the battery, fuel, foundry, refining and other chemical industries is the largest source of the lead that ends up in the environment [10]. If disposed of directly into the environment, these heavy metal contaminants can pose a very hazardous risk to living beings [11]. Additionally, the natural cycles of nature, such as food chains, can impact the distribution of these heavy metals. Utilizing degradable materials is one strategy to prevent lead pollution from becoming more prevalent in the environment. The adsorption method is one approach that has several benefits, including a relatively straightforward procedure, comparatively high effectiveness and efficiency, and the absence of hazardous side effects [12].

Recent research on adsorption methods has mainly been focused on adsorbent development. Biopolymer adsorbents have gained much attention due to their favourable properties, including being environmentally friendly, biocompatible and biodegradable [9]. Three main groups of biopolymers have been modified and investigated in many studies: natural rubber, lyocell fibre and chitosan-based sorbents [13]. Chitosan and its derivatives have been widely studied as adsorbents for heavy metal removal in wastewater treatment [9] because these materials have a high affinity for adsorbing many pollutants from aqueous solution [14]. Several studies have used modified chitosan as an adsorbent for Cd, Pb, Pd, and Pt [1], [9], [15]–[17]. To become a sorbent, chitosan must be modified as in its natural form it lacks solubility, is very fragile and has a highly rigid molecular chain [18]. This statement is supported by Qin et al. [19], who stated that chitosan only demonstrates antibacterial activity in an acidic solution, which is typically attributed to its poor solubility above pH 6.5. The structure of chitosan itself supports chemical and physical modification because of the presence of reactive hydroxyl and amino groups [20].

Carboxymethyl cellulose modified with chitosan sorbents has been commonly applied in the batch method. Unlike chitosan, carboxymethyl cellulose is easily soluble in water [21]. Hence, this difference in

solubility is typically bridged by the presence of a crosslinking agent that stabilizes the structure of both materials throughout a wider pH range. Huang et al. [22] synthesized chitosan-crosslinked graphene oxide/ carboxymethyl cellulose as an adsorbent for methylene blue, with an adsorption capacity of 3,190 mg/g. In addition, Manzoor et al. [23] used EDTA-modified chitosan-carboxymethyl cellulose to adsorb Cu(II), with an adsorption capacity of 142.95 mg/g. They also conducted another study using chitosan and carboxymethyl cellulose to synthesize arginine-cross-linked chitosan-carboxymethyl cellulose beads for the adsorption of Pb^{2+} and Cd^{2+} [9]. These prior studies utilized the batch method in their adsorption process. There are no studies available to date on this sorbent in a solid-phase extraction (SPE) method.

SPE is a preferred method for metal removal because of its simplicity [24]. The basic principle of SPE is the preconcentration of analytes from a sample solution by adsorption on the solid sorbent [25]. However, this method has a drawback: low selectivity [26]. Therefore, modification of the sorbent surface was suggested to overcome this problem [26]. Further modifications such as crosslinking may also be done to enhance the stability of the sorbent [27]. Thus, the present study aims to synthesize glutaraldehyde-cross-linked chitosan/carboxymethyl cellulose as a sorbent for Pb^{2+} adsorption using the SPE method. This sorbent was expected to have high efficiency in retaining Pb ions. In addition, we investigated SPE parameters such as pH, initial sample concentration, flow rates (loading and elution), and sorbent reusability.

EXPERIMENTAL

Materials

Materials used in this study were high molecular weight chitosan powder (Sigma-Aldrich; ≥ 75% deacetylation; Mw = 310,000-375,000 Da), carboxymethyl cellulose (Sigma-Aldrich; Mw = ~90,000 Da), glutaraldehyde 25% (Sigma-Aldrich), acetic acid, $Pb(NO_3)_2$, NaOH, HNO_3, and Na_2EDTA.

Equipment

A Fourier transform infrared spectrometer (FT-IR, Prestige-21, Shimadzu) and a scanning electron microscope-energy dispersive x-ray (SEM-EDX, JEOL JSM 6360LA Phenom-BSD Detector) were used to characterize the sorbent before and after the SPE process. An atomic absorption spectrometer (AAS, Perkin Elmer 400) was used to obtain concentration data from the sample. A digital pH meter (ATC) was used for pH adjustment. A glass column was used as a cartridge. A dosing/peristaltic pump (INTLLAB) was used to control the flow rate.

Synthesis of sorbent

The sorbent was made using three primary materials: chitosan, carboxymethyl cellulose and glutaraldehyde. Chitosan was dissolved in 80 mL of 2 % acetic acid by stirring for 2 hours. The mixture was then poured onto 1.72 grams of carboxymethyl cellulose. 100 µL of 25 % glutaraldehyde was added to the mixture which was stirred for 2 hours. The mixture was then added dropwise into 100 mL of NaOH 0.1 M solution using a syringe to form beads. These beads were then neutralized using double distilled water. The beads were dried at 50 ºC in the oven for 24 hours to obtain a dry sorbent for SPE application.

SPE Parameter Assays

The parameters tested in this study were pH, initial Pb concentration, loading and eluting flow rate and reusability. All tests used 25 mL of Pb solution, two cycles of sample loading, and 10 mL of 0.1 M Na_2EDTA as eluent. The pH testing was varied from pH 2 to 8. The Pb initial concentration was determined by conducting the SPE process at various Pb ion concentrations, namely 5, 10, 15, 20, and 25 mg L^{-1}. The loading flow rate was varied at 9, 12, 15, 18, and 21 mL min^{-1}. The same variations were also applied to the eluting flow rate tests. Finally, the reusability tests were conducted under the optimum conditions with 5 cycles of the SPE process. Figure 1 illustrates the SPE equipment setup used in this study.

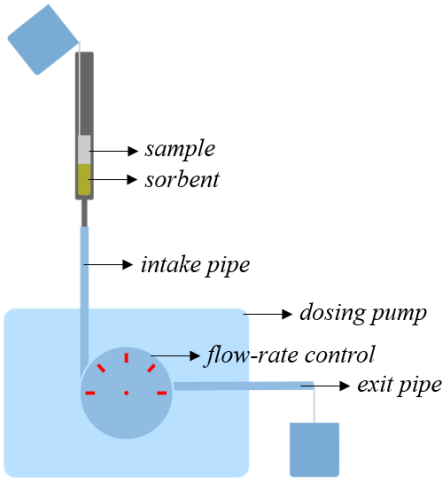

Figure 1. SPE equipment setup.

RESULTS AND DISCUSSION

FT-IR Characterization

This study successfully synthesized a sorbent from chitosan (CS) and carboxymethyl cellulose (CMC)

with glutaraldehyde (Glu) as a crosslinking agent. Glutaraldehyde was chosen as it is the most common crosslinker in the chitosan matrix due to its high stability [28]. The synthesized sorbent was characterized using FT-IR spectroscopy to study its functional groups.

Figure 2 shows the FT-IR spectra of CS, CMC, and CS-Glu-CMC. Based on Figure 2(a), the absorption peaks at 3448 and 1644 cm^{-1} indicate the N-H stretching and bending of chitosan, respectively. In addition, the broad band observed at 3456 cm^{-1} indicates the O-H stretching vibration of the hydroxyl group. The peaks at 2931 and 2889 cm^{-1} are due to the C-H stretching of chitosan. In addition, the peak at 1383 cm^{-1} corresponds to C-N stretching, and the broad band occurring around 1064 cm^{-1} was assigned to the primary alcohol C-O stretching as well as O-H bending vibrations. The spectra of CMC (Figure 2(b)) showed characteristic bands at 3447, 1603, 1318, and 1064 $cm^{-1,}$ ascribed to O-H stretching, C-O stretching of the carboxyl group, C-H bending, and C-O ether from the carboxymethyl group, respectively [29], [30]. Based on Figure 2(c), the crosslinking process shifted the peak to 3432 cm^{-1}, suggesting that the hydrogen bonding between CS and CMC was interrupted by glutaraldehyde's presence. Furthermore, the peak at 1644 cm^{-1} was not present, while a sharp peak formed at 1654 cm^{-1} due to the formation of a Schiff base (imine linkage of C=N) between the aldehyde group in glutaraldehyde and the amino group in chitosan [28]. Based on the proposed chemical structure of the sorbent (Figure 3) and examination of the spectra, the active sites that played a role in the formation of complexes with Pb^{2+} may be -N= and -OH. Table 1 summarizes the FT-IR spectral interpretation results.

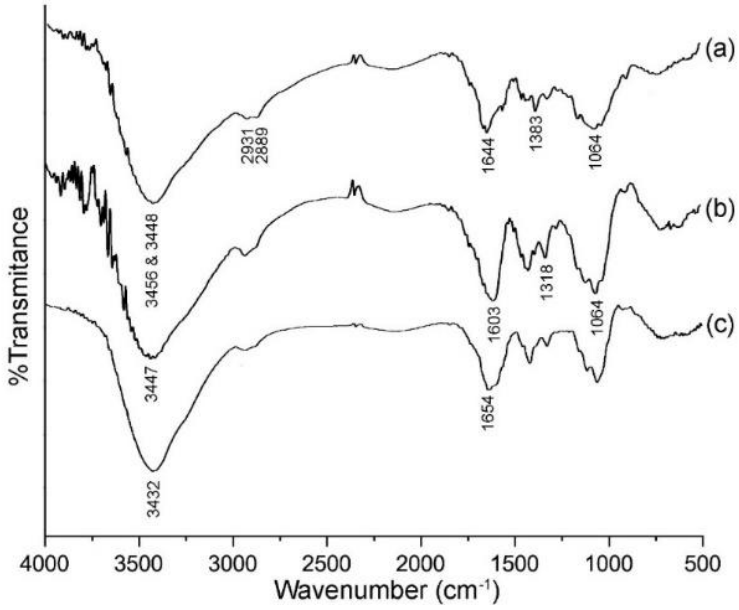

Figure 2. FT-IR spectra of (a) Chitosan (CS), (b) Carboxymethyl cellulose (CMC), and (c) Glutaraldehyde-crosslinked chitosan/carboxymethyl cellulose (CS-Glu-CMC).

Table 1. FT-IR spectral interpretation.

Wavenumber(s) (cm^{-1})	Functional groups	References
3456, 3447	O-H stretching	[31]–[34]
3448	N-H stretching	[35]
2931, 2889	C-H stretching	[36]–[39]
1654	C=N	[40]
1644	N-H bending	[41], [42]
1603	C-O stretching	[43]
1383	C-N stretching	[44]
1318	C-H bending	[45]
1064	C-O stretching, O-H bending	[46], [47]

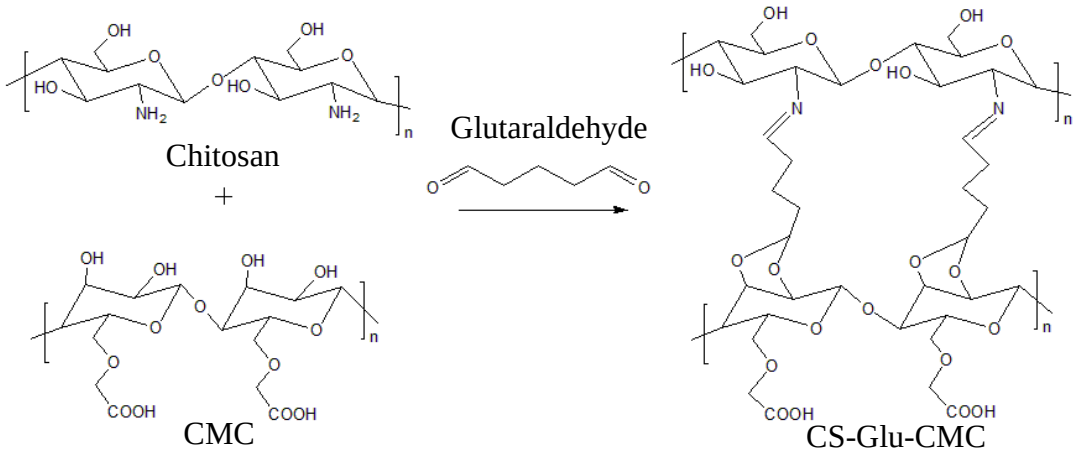

Figure 3. The proposed reaction mechanism for the formation of glutaraldehyde-crosslinked chitosan/carboxymethyl cellulose.

Figure 4 compares the FT-IR spectra of CS-Glu-CMC, the Pb-adsorbed sorbent, and the Pb-desorbed sorbent. There were some discrepancies in the functional groups of the CS-Glu-CMC sorbent owing to Pb^{2+} adsorption. The O-H stretching vibration peak in the sorbent before SPE was at 3432 cm^{-1}. However, in the Pb-adsorbed sorbent and Pb-desorbed sorbent, there was a shift in the O–H stretching vibration from 3432 to 3448 cm^{-1}. This shift occurred because Pb^{2+} ions had absorbed onto the surface of the CS-Glu-CMC, and the change in wavenumber is conceivable due to the interaction of the –OH group with Pb^{2+} ions. In addition, the CS-Glu-CMC peak of the Pb-adsorbed sorbent shifted from 1654 cm^{-1} to 1638 cm^{-1}. This is due to the interaction of Pb^{2+} ions with the nitrogen atom of the imine bond. The peak shift from 1638 cm^{-1} in the Pb-adsorbed sorbent to 1628 cm^{-1} for the desorbed sorbent was caused by the removal of Pb^{2+} ions, which were replaced by Na^{+} ions from the Na_2EDTA eluent.

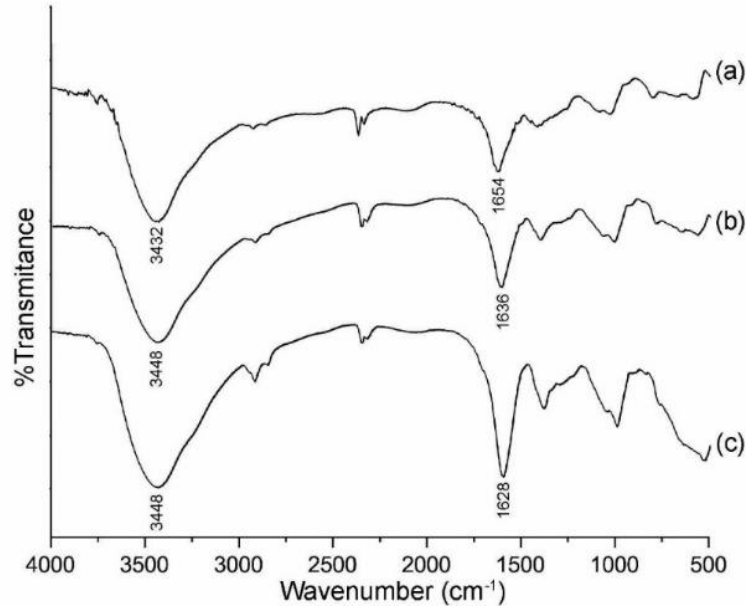

Figure 4. FT-IR spectra of (a) CS-Glu-CMC, (b) Pb-adsorbed sorbent, and (c) Pb-desorbed sorbent.

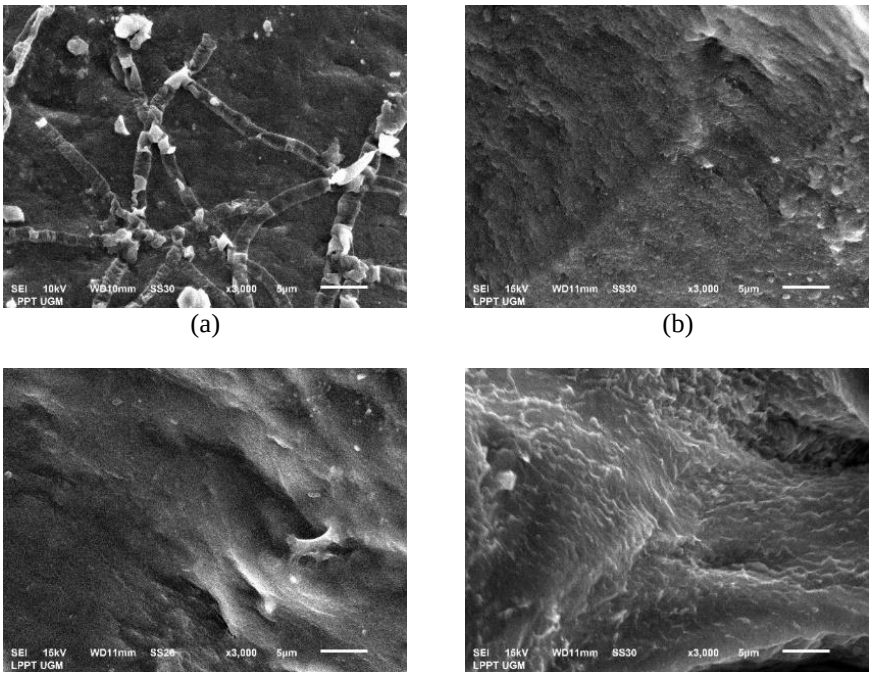

Figure 5. Morphology of the CS-Glu-CMC sorbent: (a) before SPE application, (b) during adsorption of Pb, (c) after elution, and (d) after 5 cycles of SPE (3000× magnification).

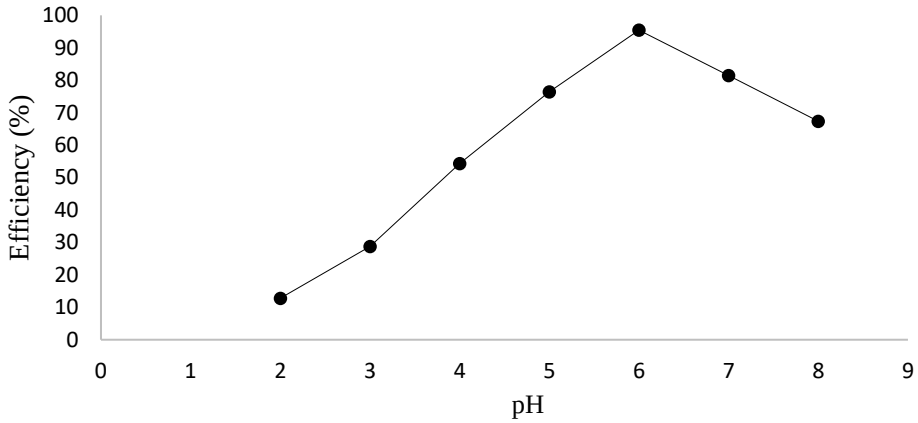

Figure 6. Effect of pH on preconcentration of Pb^{2+} using SPE.

SEM Morphology

The morphology of CS-Glu-CMC before adsorption, during adsorption, after elution, and after 5 cycles of the SPE process were analysed using SEM. The smooth surface of the CS-Glu-CMC sorbent in Figure 5(a) was due to the crosslinking reaction between chitosan and carboxymethyl cellulose [48]. However, spiral-like structures remained on the sorbent's surface, most likely due to the remaining carboxymethyl cellulose. Compared to Figure 5(b), the spiral portion was not present as it would have dissolved during the loading process due to carboxymethyl cellulose's solubility in water. Figures 5(c) and 5(d) illustrate the unevenness generated by the elution process. Figure 5(d) was more uneven than Figure 5(c) as it had been eluted five times. This indicates that the sorbent might have experienced swelling.

Effect of pH

Figure 6 illustrates the effect of pH on the pre-concentration of Pb ions using the SPE method. The efficiency (%) at various pH values showed that Pb was adsorbed optimally at pH 6, with an efficiency of 95.43 %. At pH values below 6, the excess protons in an acidic environment would have occupied the active sites of the CS-Glu-CMC, preventing Pb^{2+} ions from binding. In addition, protonation of the sorbent may also result in a decrease in efficiency [49]. As the

amount of Pb(II) adsorbed in the acid solution decreases, the amount of Pb(II) desorbed would also decrease proportionately. On the other hand, at pH > 6, the decrease in efficiency was caused by competition between OH^- ions and the sorbent in binding Pb^{2+} [49].

Effect of Initial Pb Concentration

Based on Figure 7, the highest efficiency was obtained at a concentration of 10 mg L^{-1} (93.62 %). This is because the adsorption process reached saturation at this point, reducing the sorbent's capacity to load Pb. According to Almomani et al. [50], the concentration of metal ions in wastewater affected the adsorption rate: as the concentration increased, the adsorption capacity of the adsorbent decreased. This was also corroborated by the findings of Zhang et al. [51], which indicated that the adsorbent's adsorption capacity decreased above the optimal concentration because the adsorbent's outer layer became saturated and could no longer absorb the existing metal ions.

Loading and Eluting Flow Rate

The loading and eluting flow rate test results are presented in Figure 8. Based on these results, the faster the loading flow rate, the less the adsorbed Pb. This is in line with the research by Bakircioglu et al. [52], which implied that the faster the loading flow rate, the lower the absorbance towards the analyte. At a loading flow rate of 9 mL min^{-1}, Pb would be in contact with the sorbent for longer than when other flow rates were applied. The efficiency obtained at a flow rate of 9 mL min^{-1} was 97.44 %, which was the best overall result.

The elution stage entails the exchange of analyte ions for H^+. A suitable eluent should successfully elute the analyte in a defined volume to maximize analyte recovery [53]. Na_2EDTA was chosen as the eluent in this study because Pb^{2+} has a stronger affinity to this ligand than to the sorbent. Many studies have shown that Na_2EDTA can be used effectively to recover many heavy metals from sorbents [54]. Based on Figure 8, the eluting flow rate of 9 mL min^{-1} resulted in the highest efficiency of 98.98 %. The faster the flow rate, the poorer the efficiency, as the analysis time is shortened [25]. In other words, the contact time between the eluent and the Pb^{2+} retained in the sorbent is reduced.

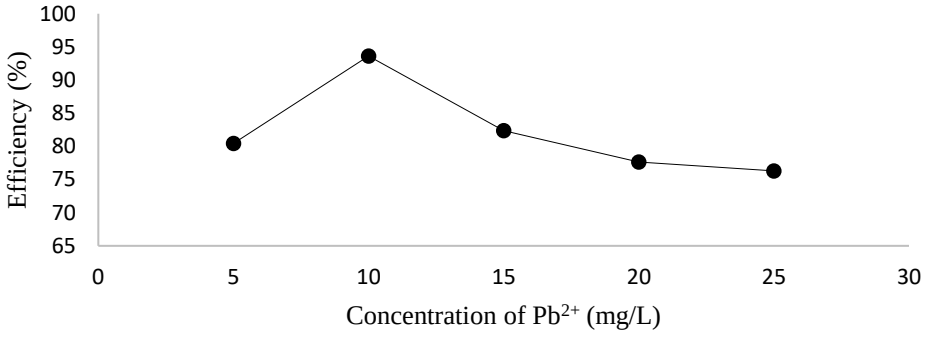

Figure 7. Effect of initial Pb concentration on SPE efficiency.

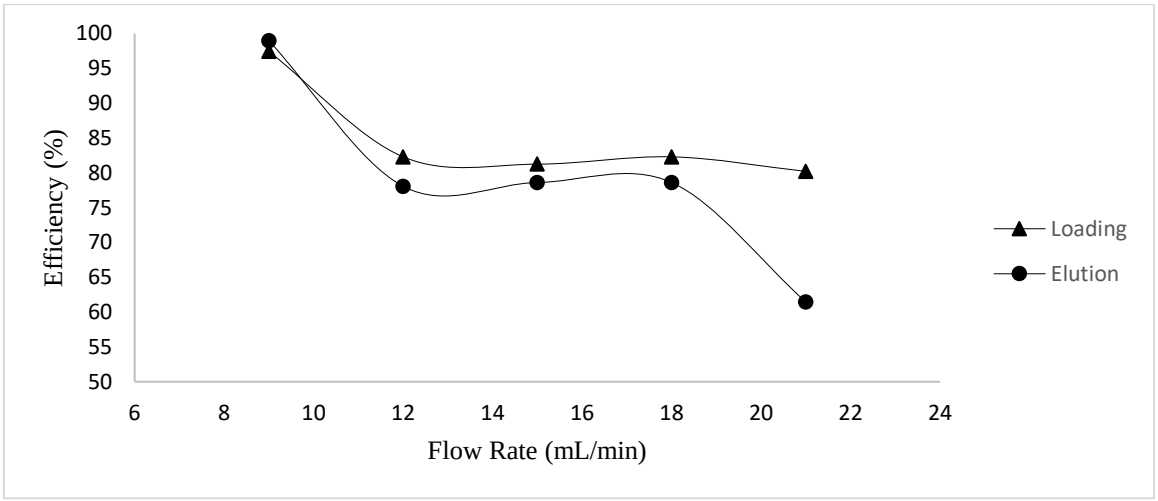

Figure 8. Effect of loading and eluting flow rate on SPE efficiency.

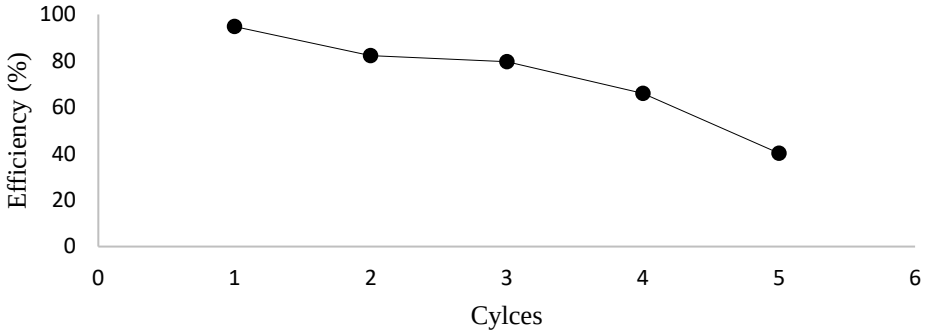

Figure 9. Effect of sorbent reusability on SPE efficiency.

Flow rate significantly impacts the amount of Pb that can be adsorbed. This is directly proportional to the contact time between Pb and the sorbent; the higher the flow rate, the shorter the contact time, and thus the lower the amount of Pb adsorbed [55]. The slower the flow rate, the longer the contact time between the eluent and the bound metal ions on the sorbent, increasing the likelihood of cation exchange.

Reusability

The recovery of metal ions while preserving sorbent efficiency through multiple reuse cycles is a critical challenge when determining the economic worth of the entire uptake process [56]. Five consecutive uptake operations were performed on the sorbent to account for the decrease in SPE efficiency. The efficiency decreased from 94.81 % to 40.22 % after five adsorption cycles (Figure 9). This may have occurred because of the swelling caused by water in the sorbent cavity during frequent use. Araújo et al. [57] reported that the polymer chains did not have time to reorganize and acquire stability by self-assembly. In addition, there were no efficient polymer entanglements that promoted disintegration and dissolution resistance.

According to Siyal et al. [58], sorbents must possess high adsorption and regeneration capacities for application in the treatment of polluted water. The adsorbent regeneration process aims to enable the adsorbent to be reused. Furthermore, regeneration aims to restore the active sites of the sorbent so that it can again bind to Pb and rearrange the groups used in the adsorption and elution processes [59]. The loss in effectiveness of the sorbent regeneration process is due to the inability of the adsorbent to absorb Pb, which renders the elution process incapable of entirely removing the complexly attached Pb from the sorbent [60].

Table 2 compares the data on Pb adsorption efficiencies of several adsorbents from prior studies. Comparisons were only made with studies that reported efficiency since the present study did not provide adsorption capacity data. In addition, there were no studies found that reported chitosan/carboxymethyl cellulose adsorption efficiencies. In order to avoid misleading comparisons, only studies focused on the adsorption efficiency of Pb are presented. Based on Table 2, the current study achieved a higher adsorption efficiency compared to previous research. In addition, the SPE method only required a short amount of time compared to the batch method. However, more research into this method is required to improve the sorbent reusability results.

Table 2. Adsorption efficiencies of Pb^{2+} in the literature.

Sorbent/Adsorbent	Efficiency	Adsorption method	References
Modified orange peel	96 %	Batch	[61]
SiO_2/graphene composite	84.23 %	Batch	[62]
Powdered activated carbon	83 %	Batch	[63]
Iron oxide magnetic nanoparticles and Ca-alginate immobilized *Phanerochaete chrysosporium*	>90 %	Batch	[64]
Glutaraldehyde-crosslinked chitosan/carboxymethyl cellulose	98.98 %	SPE	This work

CONCLUSION

The synthesis of a CS-Glu-CMC sorbent was successfully carried out through the bead formation process. The active sites on this sorbent had the potential to adsorb Pb^{2+} ions via the SPE process. The optimum SPE conditions obtained in this study were pH 6, an initial Pb concentration of 10 mg L^{-1}, and both loading and eluting flow rates of 9 mL min^{-1}. These conditions resulted in an efficiency of 98.98 %. However, the consecutive use of CS-Glu-CMC sorbent in the SPE process gave unsatisfactory results. This was because swelling occurred when the sorbent was reused, making the target metal difficult to desorb. The adsorption efficiency dropped from 94.81 % to 40.22 % after five cycles of the SPE process.

ACKNOWLEDGEMENTS

The authors would like to thank the Indonesia Endowment Fund for Education (LPDP Scholarship) for financially supporting this study.

REFERENCES

1. Masykur, A., Santosa, S. J., Siswanta, D. and Jumina (2014) Synthesis of Pb(II) imprinted carboxymethyl chitosan and the application as sorbent for Pb(II) ion. *Indonesian Journal of Chemistry*, **14(2)**, 152–159.

2. Lu, Y., Taksa, L. and Jia, H. (2020) Influence of management practices on safety performance: The case of mining sector in China. *Safety Science*, **132**, 104947.

3. Madhav, S., Ahamad, A., Singh, A. K., Kushawaha, J., Chauhan, J. S., Sharma, S. and Singh, P. (2020) Water Pollutants: Sources and Impact on the Environment and Human Health, in Advanced Functional Materials and Sensors, eds. D. Pooja, P. Kumar, P. Singh, S. Patil. *Springer, Singapore.*

4. Chen, L., Zhou, S., Shi, Y., Wang, C., Li, B., Li, Y. and Wu, S. (2018) Heavy metals in food crops, soil, and water in the Lihe River Watershed of the Taihu Region and their potential health risks when ingested. *Science of The Total Environment*, **615**, 141–149.

5. Ahmad, S. Z. N., Wan Salleh, W. N., Ismail, A. F., Yusof, N., Mohd Yusop, M. Z. and Aziz, F. (2020) Adsorptive removal of heavy metal ions using graphene-based nanomaterials: Toxicity, roles of functional groups and mechanisms. *Chemosphere*, **248**, 126008.

6. Zhang, L., Zeng, Y. and Cheng, Z. (2016) Removal of heavy metal ions using chitosan and modified chitosan: A review. *Journal of Molecular Liquids*, **214**, 175–191.

7. Türker, A. R. (2012) Separation, preconcentration and speciation of metal ions by solid phase extraction. *Separation and Purification Reviews*, **41**, 169–206.

8. Assadi, A., Fazli, M. M., Emamjomeh, M. M. and Ghasemi, M. (2016) Optimization of lead removal by electrocoagulation from aqueous solution using response surface methodology. *Desalination and Water Treatment*, **57**, 9375–9382.

9. Manzoor, K., Ahmad, M., Ahmad, S. and Ikram, S. (2019) Removal of Pb(II) and Cd(II) from wastewater using arginine cross-linked chitosan-carboxymethyl cellulose beads as green adsorbent. *RSC Advances*, **9**, 7890–7902.

10. Pan, Z. F. and An, L. (2019) Removal of Heavy Metal from Wastewater Using Ion Exchange Membranes, in Applications of Ion Exchange Materials in the Environment, eds. Inamuddin, M. Ahamed, A. Asiri. *Springer Cham.*

11. Mishra, S., Bharagava, R. N., More, N., Yadav, A., Zainith, S., Mani, S. and Chowdhary, P. (2019) Heavy Metal Contamination: An Alarming Threat to Environment and Human Health, in Environmental Biotechnology: For Sustainable Future, eds. R. Sobti, N. Arora, R. Kothari. *Springer, Singapore*.

12. Shrestha, R., Ban, S., Devkota, S., Sharma, S., Joshi, R., Tiwari, A. P., Kim, H. Y. and Joshi, M. K. (2021) Technological trends in heavy metals removal from industrial wastewater: A review. *Journal of Environmental Chemical Engineering*, **9**, 105688.

13. Zhao, M., Xu, Y., Zhang, C., Rong, H. and Zeng, G. (2016) New trends in removing heavy metals from wastewater. *Applied Microbiology and Biotechnology*, **100**, 6509–6518.

14. Vakili, M., Deng, S., Cagnetta, G., Wang, W., Meng, P., Liu, D. and Yu, G. (2019) Regeneration of chitosan-based adsorbents used in heavy metal adsorption: A review. *Separation and Purification Technology*, **224**, 373–387.

15. Dongre, R., Thakur, M., Ghugal, D. and Meshram, J. (2012) Bromine pretreated chitosan for adsorption of lead (II) from water. *Bulletin of Materials Science*, **35**, 875–884.

16. Lu, Y., He, J. and Luo, G. (2013) An improved synthesis of chitosan bead for Pb(II) adsorption. *Chemical Engineering Journal*, **226**, 271–278.

17. Asere, T. G., Mincke, S., Folens, K., Vanden Bussche, F., Lapeire, L., Verbeken, K., Van Der Voort, P., Tessema, D. A., Du Laing, G. and Stevens,

C. V. (2019) Dialdehyde carboxymethyl cellulose cross-linked chitosan for the recovery of palladium and platinum from aqueous solution. *Reactive and Functional Polymers*, **141**, 145–154.

18. Wu, M., Long, Z., Xiao, H. and Dong, C. (2016) Recent research progress on preparation and application of N, N, N-trimethyl chitosan. *Carbohydrate Research*, **434**, 27–32.

19. Qin, C., Li, H., Xiao, Q., Liu, Y., Zhu, J. and Du, Y. (2006) Water-solubility of chitosan and its antimicrobial activity. *Carbohydrate Polymers*, **63**, 367–374.

20. Pakdel, P. M. and Peighambardoust, S. J. (2018) Review on recent progress in chitosan-based hydrogels for wastewater treatment application. *Carbohydrate Polymers*, **201**, 264–279.

21. Kukrety, A., Singh, R. K., Singh, P. and Ray, S. S. (2018) Comprehension on the Synthesis of Carboxymethylcellulose (CMC) Utilizing Various Cellulose Rich Waste Biomass Resources. *Waste Biomass Valorization*, **9**, 1587–1595.

22. Huang, T., Shao, Y. -W., Zhang, Q., Deng, Y. -F., Liang, Z. -X., Guo, F. -Z., Li, P. -C. and Wang, Y. (2019) Chitosan-cross-linked graphene oxide/ carboxymethyl cellulose aerogel globules with high structure stability in liquid and extremely high adsorption ability. *ACS Sustainable Chemistry & Engineering*, **7**, 8775–8788.

23. Manzoor, K., Ahmad, M., Ahmad, S. and Ikram, S. (2019) Synthesis, Characterization, Kinetics, and Thermodynamics of EDTA-Modified Chitosan-Carboxymethyl Cellulose as Cu(II) Ion Adsorbent. *ACS Omega*, **4**, 17425–17437.

24. Pourjavid, M. R., Arabieh, M., Sehat, A. A., Rezaee, M., Hosseini, M. H., Yousefi, S. R. and Jamali, M. R. (2014) Flame atomic absorption spectrometric determination of Pb(II) and Cd(II) in natural samples after column graphene oxide-based solid phase extraction using 4-acetamido-thiophenol. *Journal of the Brazilian Chemical Society*, **25**, 2063–2072.

25. He, Q., Yang, D., Deng, X., Wu, Q., Li, R., Zhai, Y. and Zhang, L. (2013) Preparation, characterization and application of N-2-Pyridylsuccinamic acid-functionalized halloysite nanotubes for solid-phase extraction of Pb(II). *Water Research*, **47(12)**, 3976–3983.

26. Wang, Q., Chang, X., Hu, Z., Li, D. and Tu, Z. (2012) Solid-phase extraction and preconcentration of trace Pb(II) from water samples with folic acid modified silica gel. *International Journal of Environmental Analytical Chemistry*, **92(11)**, 1289–1301.

27. Luo, W., Bai, Z. and Zhu, Y. (2017) Comparison of Co(II) adsorption by a crosslinked carboxymethyl chitosan hydrogel and resin: Behaviour and mechanism. *New Journal of Chemistry*, **41(9)**, 3487–3497.

28. Gan, P. G., Sam, S. T., Abdullah, M. F., Omar, M. F. and Tan, W. K. (2020) Comparative study on the properties of cross-linked cellulose nanocrystals/chitosan film composites with conventional heating and microwave curing. *Journal of Applied Polymer Science*, **137(48)**, 1–14.

29. Baek, M. -H., Ijagbemi, C. O., O, S. -J. and Kim, D. -S. (2010) Removal of Malachite Green from aqueous solution using degreased coffee bean. *Journal of Hazardous Materials*, **176(1–3)**, 820–828.

30. Siswanta, D., Wahyuni, R. and Mudasir, M. (2020) Synthesis of glutaraldehyde-crosslinked carboxymethyl cellulose-polyvinyl alcohol film as an adsorbent for methylene blue. *Key Engineering Materials*, **840**, 35-42.

31. Boukaoud, A., Chiba, Y. and Sebbar, D. (2021) A periodic DFT study of IR spectra of amino acids: An approach toward a better understanding of the N-H and O-H stretching regions. *Vibrational Spectroscopy*, **116**, 103280.

32. Eprasatya, A., Yulizar, Y., Yunarti, R. T. and Apriandanu, D. O. B. (2020) Fabrication of Gd_2O_3 nanoparticles in hexane-water system using Myristica fragrans Houtt leaves extract and their photodegradation activity of malachite green. *IOP Conference Series: Materials Science and Engineering*, **902(1)**, 012004.

33. Jose, A., Nivitha, M. R., Krishnan, J. M. and Robinson, R. G. (2020) Characterization of cement stabilized pond ash using FTIR spectroscopy. *Construction and Building Materials*, **263**, 120136.

34. Qian, T., Li, J., Min, X., Deng, Y., Guan, W. and Ning, L. (2015) Diatomite: A promising natural candidate as carrier material for low, middle and high temperature phase change material. *Energy Conversion and Management*, **98**, 34–45.

35. Nguyen, T. K. L., Nguyen, N. D., Dang, V. P., Phan, D. T., Tran, T. H. and Nguyen, Q. H. (2019) Synthesis of platinum nanoparticles by gamma Co-60 ray irradiation method using chitosan as stabilizer. *Advances in Materials Science and Engineering*, 1–5.

36. Ravindran, B., Shiny, R. A., Beno, T. B. and Lavanya, N. (2021) Influence of sodium bromide on the growth of succinic acid crystal. *Materials Today: Proceedings*.

37. Reza, M. S., Taweekun, J., Afroze, S., Siddique, S. A., Islam, M. S., Wang, C. and Azad, A. K. (2023) Investigation of Thermochemical Properties and Pyrolysis of Barley Waste as a Source for Renewable Energy. *Sustainability*, **15(2)**, 1643.

38. Beikzadeh, S., Hosseini, S. M., Mofid, V., Ramezani, S., Ghorbani, M., Ehsani, A. and Mortazavian, A. M. (2021) Electrospun ethyl cellulose/poly caprolactone/gelatin nanofibers: The investigation of mechanical, antioxidant, and antifungal properties for food packaging. *International Journal of Biological Macromolecules*, **191**, 457–464.

39. Awitdrus, A., Putri, M. S. D., Syahputra, R. F., Iwantono, I. and Saktioto, S. (2021) Activated Carbon Based on Pineapple Crown for Heavy Metal Adsorption. *Advanced Materials Research*, **1162**, 57–64.

40. Chellaian, J. D. and SS, S. R. (2021) Co (II), Ni (II), Cu (II), and Zn (II) complexes of 4-amino-antipyrine-derived Schiff base. Synthesis, structural elucidation, thermal, biological studies, and photocatalytic activity. *Journal of Heterocyclic Chemistry*, **58(4)**, 928–941.

41. Zhan, J., Morsi, Y., Ei-Hamshary, H., Al-Deyab, S. S. and Mo, X. (2016) Invitro evaluation of electrospun gelatin–glutaraldehyde nanofibers. *Frontiers of Materials Science*, **10(1)**, 90–100.

42. Priya, S. S., Balakrishnan, K., Surendran, P., Lakshmanan, A., Geetha, P., Rameshkumar, P., Hegde, T. A., Vinitha, G. and Raj, A. A. (2021) Investigations on structural, mechanical, optical, electrical, third-order nonlinear optical and antibacterial activity of 4-aminopyridine monophthalate single crystal. *Journal of Electronic Materials*, **50**(1), 291–302.

43. Lehto, J., Louhelainen, J., Huttunen, M. and Alén, R. (2017) Spectroscopic analysis of hot-water- and dilute-acid-extracted hardwood and softwood chips. *Spectrochimica Acta Part A: Molecular and Biomolecular Spectroscopy*, **184**, 184-190.

44. Ariyanta, H. A., Ivandini, T. A. and Yulizar, Y. (2021) Novel NiO nanoparticles via phytosynthesis method: Structural, morphological and optical properties. *Journal of Molecular Structure*, **1227**, 129543.

45. Marques, A. S., Moraes, E. P., Júnior, M. A., Moura, A. D., Neto, V. F., Neto, R. M. and Lima, K. M. (2015) Rapid discrimination of Klebsiella pneumoniae carbapenemase 2–producing and non-producing Klebsiella pneumoniae strains using near-infrared spectroscopy (NIRS) and multivariate analysis. *Talanta*, **134**, 126–131.

46. Maulida, M., Siagian, M. and Tarigan, P. (2016) Production of starch based bioplastic from cassava peel reinforced with microcrystalline celllulose avicel PH101 using sorbitol as plasticizer. *Journal of Physics: Conference Series*, **710(1)**, 012012.

47. Monika, M., Dhar, P. and Katiyar, V. (2017) Thermal degradation kinetics of polylactic acid/acid fabricated cellulose nanocrystal based bio-nanocomposites. *International Journal of Biological Macromolecules*, **104**, 827–836.

48. Igberase, E. and Osifo, P. (2015) Equilibrium, kinetic, thermodynamic and desorption studies of cadmium and lead by polyaniline grafted cross-linked chitosan beads from aqueous solution. *Journal of Industrial and Engineering Chemistry*, **26**, 340–347.

49. Sobhi, H. R., Mohammadzadeh, A., Behbahani, M. and Esrafili, A. (2019) Implementation of an ultrasonic assisted dispersive μ-solid phase extraction method for trace analysis of lead in aqueous and urine samples. *Microchemical Journal*, **146**, 782–788.

50. Almomani, F., Bhosale, R., Khraisheh, M., Kumar, A. and Almomani, T. (2020) Heavy metal ions removal from industrial wastewater using magnetic nanoparticles (MNP). *Applied Surface Science*, **506**, 144924.

51. Zhang, J., Xiong, Z., Li, C. and Wu, C. (2016) Exploring a thiol-functionalized MOF for elimination of lead and cadmium from aqueous solution. *Journal of Molecular Liquids*, **221**, 43–50.

52. Bakircioglu, Y., Segade, S. R., Yourd, E. R. and Tyson, J. F. (2003) Evaluation of Pb-Spec® for flow-injection solid-phase extraction preconcentration for the determination of trace lead in water and wine by flame atomic absorption spectrometry. *Analytica Chimica Acta*, **485(1)**, 9–18.

53. Savio, M., Parodi, B., Martinez, L. D., Smichowski, P. and Gil, R. A. (2011) On-line solid phase extraction of Ni and Pb using carbon nanotubes and modified carbon nanotubes coupled to ETAAS. *Talanta*, **85(1)**, 245–251.

54. Deng, L., Su, Y., Su, H., Wang, X. and Zhu, X. (2006) Biosorption of copper (II) and lead (II) from aqueous solutions by nonliving green algae Cladophora fascicularis: Equilibrium, kinetics and environmental effects. *Adsorption*, **12(4)**, 267–277.

55. Fang, X., Li, J., Li, X., Pan, S., Zhang, X., Sun, X., Shen, J., Han, W. and Wang, L. (2017) Internal pore decoration with polydopamine nanoparticle on polymeric ultrafiltration membrane for enhanced heavy metal removal. *Chemical Engineering Journal*, **314**, 38–49.

56. Elsayed, N. H., Alatawi, A. and Monier, M. (2020) Diacetylmonoxine modified chitosan derived ion-imprinted polymer for selective solid-phase extraction of nickel (II) ions. *Reactive and Functional Polymers*, **151**, 104570.

57. Araújo, L. D. C. B., de Matos, H. K., Facchi, D. P., de Almeida, D. A., Gonçalves, B. M. G., Monteiro, J. P., Martins, A. F. and Bonafé, E. G. (2021) Natural carbohydrate-based thermosensitive chitosan/pectin adsorbent for removal of Pb(II) from aqueous solutions. *International Journal of Biological Macromolecules*, **193**, 1813–1822.

58. Siyal, A. A., Shamsuddin, M. R., Low, A. and Rabat, N. E. (2020) A review on recent developments in the adsorption of surfactants from wastewater. *Journal of Environmental Management*, **254**, 109797.

59. Ajao, V., Nam, K., Chatzopoulos, P., Spruijt, E., Bruning, H., Rijnaarts, H. and Temmink, H. (2020) Regeneration and reuse of microbial extracellular polymers immobilised on a bed column for heavy metal recovery. *Water Research*, **171**, 115472.

60. Luo, J., Yu, D., Hristovski, K. D., Fu, K., Shen, Y., Westerhoff, P. and Crittenden, J. C. (2021) Critical Review of Advances in Engineering Nanomaterial Adsorbents for Metal Removal and Recovery from Water: Mechanism Identification and Engineering Design. *Environmental Science & Technology*, **55(8)**, 4287–4304.

61. Lasheen, M. R., Ammar, N. S. and Ibrahim, H. S. (2012) Adsorption/desorption of Cd (II), Cu (II) and Pb (II) using chemically modified orange peel: Equilibrium and kinetic studies. *Solid State Sciences*, **14(2)**, 202–210.

62. Hao, L., Song, H., Zhang, L., Wan, X., Tang, Y. and Lv, Y. (2012) SiO_2/graphene composite for highly selective adsorption of Pb(II) ion. *Journal of Colloid and Interface Science*, **369**(1), 381–387.

63. Abudaia, J. A., Sulyman, M. O., Elazaby, K. Y. and Ben-Ali, S. M. (2013) Adsorption of Pb(II) and Cu(II) from aqueous solution onto activated carbon prepared from dates stones. *International Journal of Environmental Science and Development*, **4(2)**, 191.

64. Xu, P., Zeng, G. M., Huang, D. L., Lai, C., Zhao, M. H., Wei, Z., Li, N. J., Huang, C. and Xie, G. X. (2012) Adsorption of Pb(II) by iron oxide nanoparticles immobilized Phanerochaete chrysosporium: equilibrium, kinetic, thermodynamic and mechanisms analysis. *Chemical Engineering Journal*, **203**, 423–431.